www.czasopisma.pan.pl PAN www.journals.pan.pl

ARCHIVES of FOUNDRY ENGINEERING

ISSN (2299-2944)
Volume 18
Issue 1/2018

129 – 134

DOI: 10.24425/118825

24/1

Published quarterly as the organ of the Foundry Commission of the Polish Academy of Sciences

A Study of Inclusions in Aluminum and Titanium Deoxidized 4130

R.B. Tuttle *, S. Kottala
Saginaw Valley State University, 209 Pioneer Hall,
7400 Bay Rd., 48710 University Center, United States
* Corresponding author. E-mail address: rtuttle@svsu.edu

Received 02.10.2017; accepted in revised form 14.11.2017

Abstract

In this paper, the authors investigated the size distribution of titanium oxide (TiO_2), titanium nitride (TiN) and titanium carbide (TiC) inclusions in a titanium deoxidized 4130 steel and compared it with the 4130 base alloy composition inclusions. TiN and TiC inclusions are of particular interest due to their role as heterogeneous nuclei for various phase reactions in steels. Two types of samples were prepared, a polished sample and a filtered sample. Electrolytic dissolution was employed to make the filter paper samples. The size range of titanium inclusions was found to be more than that of the non-metallic inclusions from 4130 base alloy heat. Titanium inclusions from the filter and polished samples were round in shape. TiC and TiN inclusions were not found in the electrolytic extraction samples. Inclusions and their chemistries were analyzed using scanning electron microscope and energy dispersive spectrometer. The inclusion size range was larger for the titanium deoxidized samples than the base alloy. However, in both steels the majority of inclusions had a size smaller than 10 μm.

Keywords: Steel, Sand casting, Inclusions, Electrolytic extraction, Inclusion characterization

1. Introduction

In 1990, the expression "Oxide Metallurgy" was initially used to depict the idea that oxides with a size from submicron to a few microns are utilized as nucleation sites for phase transformations. Afterward, researchers realized that not only oxide inclusions, but also sulfide, nitride, and carbide inclusions can have an impact on the microstructure, so the more correct term "Inclusion Engineering" was adopted.

As has been generally known for years, most inclusions are detrimental to mechanical properties. However, as stated earlier, there has been a realization that some inclusions can be beneficial to metals [1]. In particular, titanium containing inclusions can play a role in phase transformations. Some act as heterogenous nuclei during solidification [2]. Others have been observed to affect the eutectoid reaction and cause the formation of acicular ferrite [3]. Both routes result in a finer microstructure and higher mechanical properties. Thus, titanium inclusions are of interest to industry.

According to the theory advanced by Turnbull and Vonnegut, a nucleating phase will be effective in promoting nucleation when the lattice parameters in the low-index crystallographic planes of both the substrate and the nucleated solid are similar [2]. TiN and TiC are compounds with the cubic rock-salt type of structure and have respective disregistries of 3.9 % and 5.9 % with δ-ferrite [2]. Bramfitt conducted experiments with these compounds and determined that they reduce the undercooling required for solidification and confirmed Turnbull and Vonnegut's theory [2]. Therefore, purposely creating these phases during solidification could increase the number of dendrites that form and reduce the grain size, which will improve the strength and ductility.

Intragranular ferrite is known to provide an optimal combination of high strength and increased toughness due to its

refined grain size and interlocking microstructure. Thus, its formation provides a route for improved mechanical properties of steel. It has been reported that intragranular ferrite nucleates mainly at the surface of non-metallic inclusions [3]. Secondary nucleation of intragranular ferrite occurs through sympathetic nucleation from the ferrite laths [4]. Titanium nitride (TiN) has been observed to be effective in initiating the nucleation of intragranular ferrite [5]. Nucleation of intragranular ferrite has also been observed on aluminum rich inclusions [6]. Manganese sulfide (MnS) has proved to be an effective nuclei [7]. Titanium oxide (TiO_2) inclusions appear to be effective in stimulating the formation of intragranular ferrite [8,9]. All these inclusions work as the heterogeneous nucleation sites of ferrite during the eutectoid reaction. Among them, TiO_2 has been found to be one of the most effective phases. Therefore, understanding the shift in inclusion types, particularly titanium containing ones, is a significant step in the development of steel grain refiners.

Goto et al. investigated the effect of the cooling rate on composition of oxides precipitated during solidification of titanium deoxidized steel. The composition and size of the oxides in the continuously cast steels were examined and theoretically analyzed [10,11]. The oxides mainly consisted of Ti_2O_3, Al_2O_3, and MnO. The Ti_2O_3 content increases and Al_2O_3 content decreases with decrease in the cooling rate during solidification in the case of inclusions whose diameter is less than 10 µm. On the other hand, the composition of oxides whose diameter was larger than 10 µm does not change with the cooling rate. When the size of oxide is smaller, the effect of cooling rate on oxide compositions was remarkable [10,11]. The Ti_2O_3 content in the oxide inclusions at the end of solidification increased with a decrease in the oxide diameter before solidification and a decrease in the cooling rate during solidification. From the theoretical analysis, the changes in composition and diameter were due to oxide growth during solidification [10,11].

Wang et al. examined the addition of a Fe-Ti-N master alloy to refine the structure of 409L ferritic stainless steel [12]. The master alloy was created by melting an iron, 5 wt. % titanium mixture under a controlled atmosphere. Upon complete melting, nitrogen was added to the furnace environment to cause the formation of TiN particles [12]. This master alloy was then added to batches of 409L steel at a rate of 0 to 2.5 wt.%. They observed that the equiaxed zone increased from 14% of the overall microstructure to 100%. The grain size decreased from 1503 µm to 303 µm [12].

Park et al. examined complex inclusions and their effect on the solidification structure of a Fe-Ni-Mn-Mo alloy [13]. They examined the role aluminum, cerium, magnesium, and titanium additions had on the solidification structure. All additions were only exampled at the 0.2 wt. % level. The titanium-aluminum batches contained simple Al_2O_3 and TiN inclusions, which did not significantly refine the solidification structure [13]. The magnesium-titanium specimen produced the finest solidification structure and complex $MgO(MgAl_2O_4)$-TiN appeared to form. Some TiN inclusions were also observed [13].

More recently, the use of complex inclusion precipitation reactions have been examined to promote the formation of TiN inclusions [14]. Lekakh et al. experimented with a series of aluminum, magnesium, and then titanium additions. The concept was to form Al_2MgO_4 inclusions which would then act as nuclei for TiN inclusisons. The TiN inclusions would in turn assist the formation of primary dendrites in a Cr-Ni-Mo stainless steel casting. Examination of the industrial casting under test found a large decrease in the grain size and columnar zone [14]. The desired sequential formation of the inclusions was confirmed by transmission electron microscopy [14]. A similar approach has been reported by other researchers [13,15, 16, 17].

To assist in understanding the formation of titanium containing inclusions, the work presented in this paper examined a batch of aluminum deoxidized steel and a titanium deoxidized steel. The focus was primarily on how inclusion types and size distributions shifted between these two deoxidizers.

2. Materials and methods of investigation

Fifty kilogram heats of 4130 were melted in a 3kHz high frequency induction furnace. The heats were tapped into a ladle at a melt temperature of 1732ºC ± 10ºC and then poured into plate castings at a pouring temperature of 1593ºC ± 10ºC using green sand molds. During tapping, the aluminum shot or ferrotitanium was added to the stream. A series of 23 mm by 142 mm by 209 mm plate castings were produced as part of this work (See Fig. 1). This plate geometry has been created by the authors' lab to provide samples free from microporosity while being efficient in the use of the amount of steel. Table 1 lists the chemical composition of each batch poured.

The molds cooled for one hour prior to shakeout to ensure that the cooling rate through the eutectoid reaction would be the same for each casting. Samples were taken from each batch to determine the chemical composition by using an optical emission spectrometer (OES) (See Fig. 1). Metallographic samples were prepared using SiC paper, polycrystalline diamond, and alumina polishing compounds.

Table 1.
Composition of each batch

Sample	C (wt. %)	Si (wt. %)	Mn (wt. %)	P (wt. %)	S (wt. %)	Cr (wt. %)	Ti (wt. %)	Al (wt. %)
4130-Base alloy	0.308	0.156	0.453	0.010	0.013	0.989	0.002	0.141
4130- Ti Deoxidized	0.295	0.217	0.442	0.011	0.013	0.908	0.08	0.006

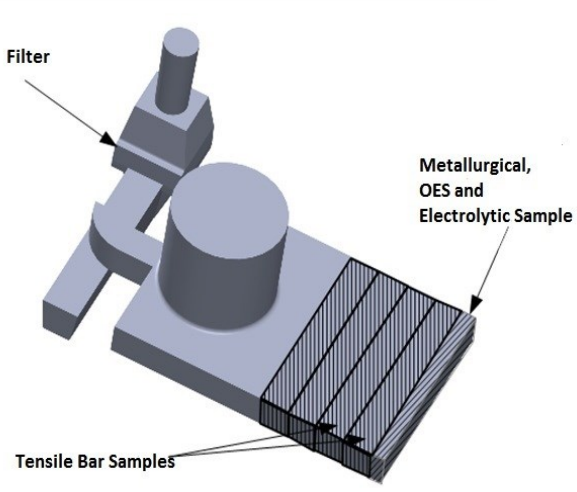

Fig. 1. Plate casting geometry and sample locations

Filter paper samples were prepared by an electrolytic dissolution technique that used a 2% TEA (2 v/v% triethanolamine-1w/v% tetramethylammonium-remainder methanol) solution as an electrolyte. Electrolysis was controlled with a constant current rate (40-45mA) and a voltage of 3-3.5 V to obtain a stable dissolution rate [18]. For the dissolution process, a steel sample was sectioned to a length of 10 mm, width of 15 mm, and height of 15 mm. A total of two samples were sectioned from the two different heats named 4130 with base alloy and titanium deoxidizer. The sectioned samples were weighed and cleaned in an ultrasonic bath and rinsed in acetone before dissolving. Details of the sample preparation are given in a previous paper [18]. After electrolytic dissolution, each sample was subjected to ultrasonic cleaning in a 60 ml methanol bath and then the solution containing non-metallic inclusions were filtered through a polycarbonate (PC) membrane film filter having a 0.05 µm open-pore diameter using vacuum filtration glassware. The filter paper was then placed on a watch glass and rinsed with the methanol before drying for 12 hours. Using a scanning electron microscope (SEM) stub with double sided carbon tape on it, inclusions were collected from the center of the filter paper.

The SEM was used to analyze the filtered and polished samples from the 4130 base alloy and Ti deoxidized samples. For the polished samples, 100 inclusions from each batch were examined using an energy dispersive spectrometer (EDS). The same method was employed on the filter paper samples, but only 10 to 20 inclusions from each batch were characterized. The filter paper samples were analyzed to ensure accurate chemistries were obtained for the inclusions by eliminating the matrix and to assist in properly characterizing the inclusion shape.

3. Description of achieved results of own researches

In the filter paper samples, only TiO_2 inclusions were identified, and the average size was found to be 6.29 µm whereas the average size of the TiO_2 inclusions from the polished samples is 9.9 µm. This might indicate that TiO_2 inclusions are not stable during electrolytic dissolution. The lack of TiC and TiN inclusions in the filter paper samples certainly suggest that they dissolved during electrolytic extraction. Characterizing these inclusions was only possible in the polished samples.

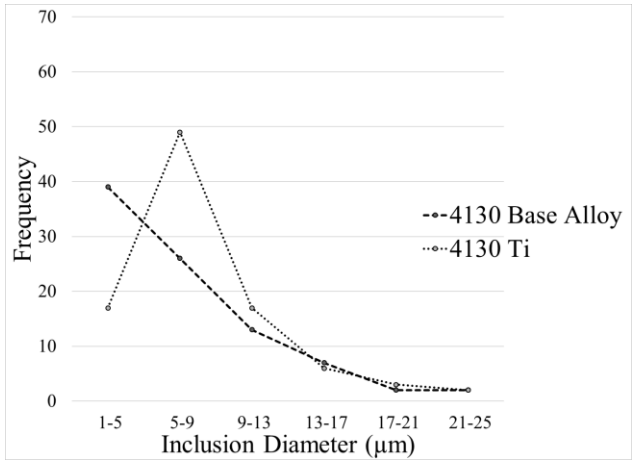

Fig. 2. Overall inclusion size range from 4130 Ti deoxidized steel and base alloy

As shown in Fig. 2, the highest percentage of inclusions for the 4130 base alloy sample lay in the 1-5 µm size range whereas the highest percentage of inclusions in the 4130 Ti deoxidized batch took place in the 5-9 µm size range. Titanium deoxidation appears to produce a slightly larger inclusion.

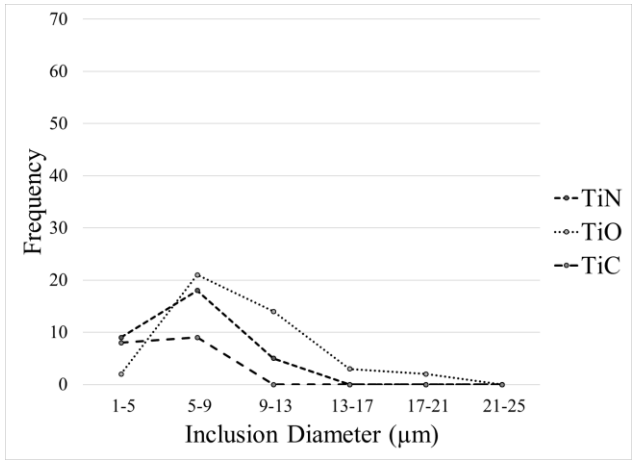

Fig. 3. Size range for different titanium inclusions

The TiN, TiC, and TiO_2 inclusions found in the 4130 Ti deoxidized batch had very similar size distributions (See Fig. 3).

As indicated in Fig. 4, the percentage of TiO_2 inclusions was found to be over 40%. TiN inclusions made up around 32% of the inclusion population, and TiC inclusions were only around 10% of the population. Figure 5 shows that FeAlO and MnS percentages in 4130 base alloy batch were much higher than that of the 4130 Ti deoxidized steel. TiC and TiN inclusions were found to be surrounded by MnS inclusions in the 4130 Ti deoxidized sample. This may have caused the reduction of MnS

inclusion population in 4130 Ti deoxidized because the MnS was classified as a TiN or TiC inclusion. In the case of the FeAlO inclusions, the 4130 Ti deoxidized batch had a smaller percentage. The FeAlO inclusion population fraction was 3% in the 4130 Ti deoxidized steel. It was 42% in the 4130 base alloy. This may indicate that the titanium worked more efficiently as a deoxidizer during casting. FeAlO inclusions typically form due to reoxidation of the steel during pouring. The iron pickup in these inclusions happens as a result of the aluminum in the melt being depleted locally. It appears that the titanium addition was sufficient to prevent the formation of reoxidation inclusions of this type.

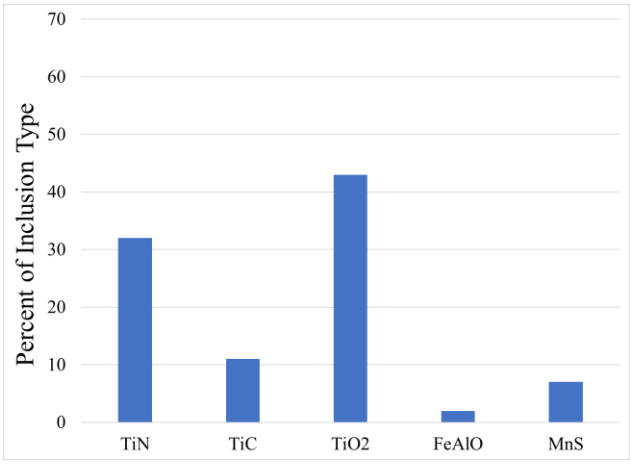

Fig. 4. Fraction of inclusion types from 4130 Ti deoxidized steel

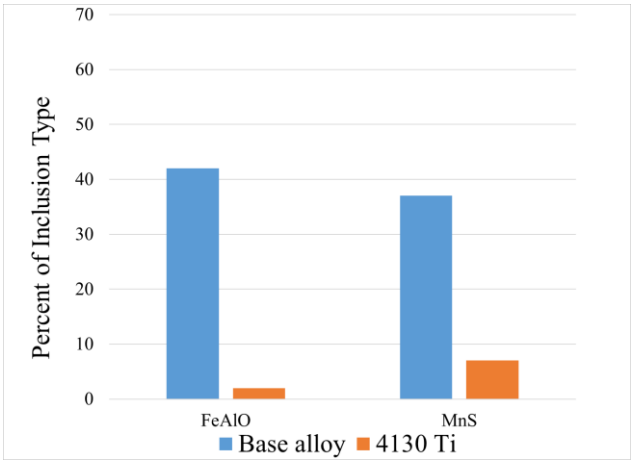

Fig. 5. FeAlO and MnS inclusions from 4130 Ti deoxidized and base alloy steel

There was also a difference in the measured MnS inclusion population fraction in the 4130 Ti deoxidized steel. It was only 6.5%, whereas in the 4130 base alloy it was 32%. TiN and TiC inclusions act as nuclei for MnS formation since it forms after solidification. Upon solidification and cooling to room temperature, manganese and sulfur from the surrounding steel matrix diffuse to TiC and TiN inclusions to form MnS [13]. This matches with the observation that the TiN and TiC inclusions were surrounded by MnS. Thus, the MnS inclusion percentage in Ti deoxidized steel was found to be less when compared to base alloy steel because the inclusions were classified primarily as TiC or TiN. The epitaxial growth of MnS on the TiC and TiN inclusions may also explain the slightly larger inclusion size found in the size distributions. The growth of MnS on existing inclusions would cause their measured size to be larger.

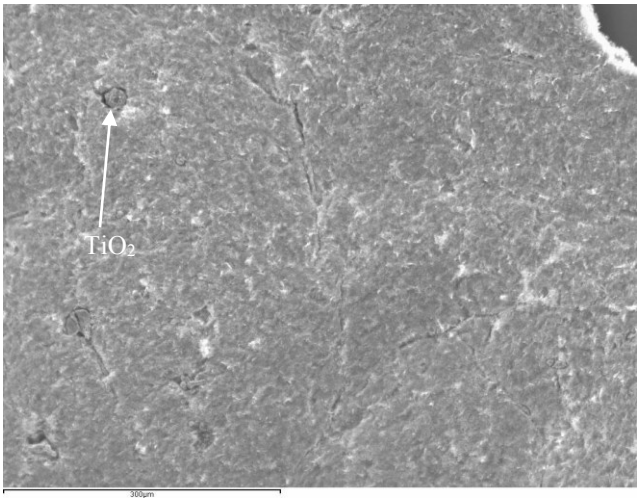

Fig. 6. TiO_2 inclusion from a filter paper sample if 4130 Ti

Table 2.
TiO_2 inclusion from a filter paper sample

Element	Weight %
Ti	40.00
O	34.52
N	11.49

Fig. 6 depicts that the TiO_2 inclusion from the filter paper sample were found to be round. The TiO_2 inclusions were found to be round in the polished samples also. The TiC and TiN inclusions were not found in the filtered paper samples. This indicates that TiC and TiN are probably not stable in the electrolytic dissolution process. Polished samples of 4130 Ti deoxidized batch analyzed in the SEM with EDS provided data on TiN and TiC inclusions. Fig. 7 and 8 depict the TiN and TiC inclusions found in the polished samples of the 4130 Ti deoxidized batch steel. The TiN and TiC inclusions had a faceted structure.

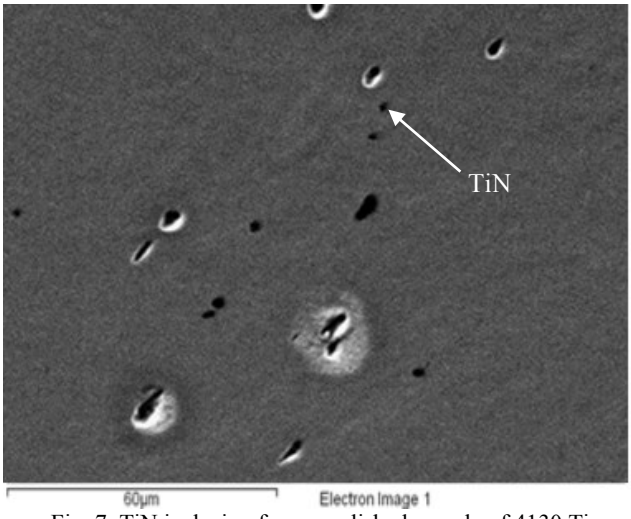

Fig. 7. TiN inclusion from a polished sample of 4130 Ti

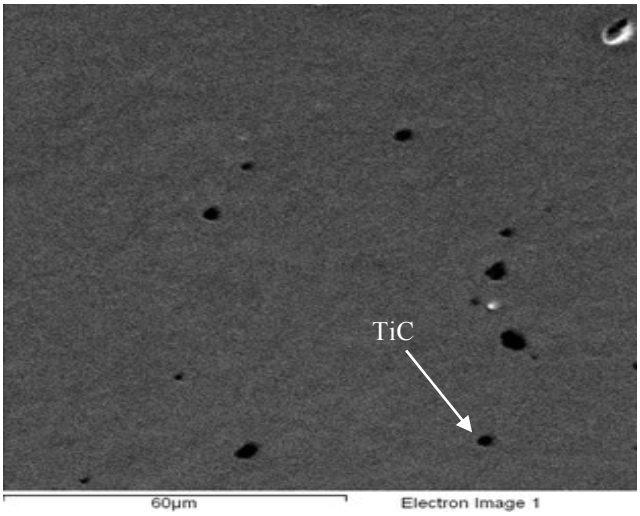

Fig. 8. TiC inclusion from a polished sample of 4130 Ti

4. Conclusions

This work observed several differences between the inclusions formed. Forty percent of the overall inclusions from 4130 base alloy were between 1-5 µm whereas 50% of overall inclusions from the 4130 Ti deoxidizer batch were between 5-9 µm. The TiN and TiC inclusions in the titanium deoxidized steel were surrounded by MnS. This likely caused the slightly larger inclusion size in the Ti deoxidized steel. No TiN and TiC inclusions were noted in the samples which were prepared through the electrolytic dissolution process. This phenomenon indicated that TiN and TiC inclusions are dissolved during this process, and it is an inappropriate technique for quantifying their size and three-dimensional morphology. Many of the inclusions appeared the same size in the filtered samples and polished samples. Titanium bearing inclusions appeared round in both the filter and polished samples. Forty-two percent of the inclusions in the titanium deoxidized steel were TiO_2 type inclusions; TiN inclusions formed the next largest group at 30%. FeAlO and MnS inclusion formation was much smaller in the titanium deoxidized steel than the base alloy.

Acknowledgements

The authors would like to thank the support of the Office of Naval Research who financially support this work through Award Number N141410740. FOSECO's support through donations of ladle liners is also acknowledged. Taylor Hunter, Aaron O'Neal, and Tyler Schramski are also recognized for their assistance in pouring the test castings. Jennie Tuttle also deserves recognition for her editorial assistance.

References

[1] Tuttle, R.B. (2012). *Foundry Engineering: The Metallurgy and Design of Castings*. Charleston, SC. Createspace Independent Publishing.
[2] Bramfitt, B. (1979). The effect of carbide and nitride additions on the heterogeneous nucleation behavior of liquid iron. *Metallurgical Transactions.* 1, 1987-1995.
[3] Farrar, R.A. & Harrison, P.L. (1987). Acicular ferrite in carbon-manganese weld metals: an overview. *Journal of Materials Science.* 22, 3812-3820.
[4] Barbaro, F.J., Krauklis, P. & Easterling, K.E. (1989). The formation of aciculart ferrite at oxide particles in steels. *Materials Science and Technology.* 5(11), 1057-1068.
[5] Kanazawa, S., Nakashima, A., Okamoto, K. & Kanaya, K. (1976). Improvement of weld fusion zone toughness by find TiN. *Transactions of the Iron and. Steel Institute of Japan.* 16(9), 486-495.
[6] Bhatti, A.R., Saggese, M.E., Hawkins, D.N., Whiteman, J.A., & Goding, M.S. (1984). Analysis of inclusions in submerged arc welds in microalloyed steels. *Welding Journal.* 63, 224-230.
[7] Abson, D.J., Dolby, R.E., & Hart, P.H.M. (1978). The role of non-metallic inclusions in ferrite nucleation in carbon steel weld metals. *Trends in Steels and Consumable for Welding*. 75-101.
[8] Homma, H. Ohkita, S., Matsuda, S. & Yamamoto, K. (1987). Improvement of haz toughness in hsla steel by introducing finely dispersed ti-oxide. *Welding Journal.* 66, 301-309.
[9] Lee, J.L. & Pan, Y.T. (1991). Development of tio_x- bearing steels with superior batch effected zone toughness. *Met. Trans. A.* 22A, 2818-2822.
[10] Goto, H., Miyazawa, K., Yamada, K. & Tanaka, K. (1995). Effect of cooling rate on composition of oxides precipitated druing solidification of steels. *ISIJ International.* 35(6), 708-714.
[11] Goto, H., Miyazawa, K., Yamagishi, K., Ogibayahsi, S. & Tanaka, K. (1994). Effect of cooling rate on oxide precipitation during solidification of low-carbon steels. *ISIJ International.*. 34(5), 414-419.

[12] Wang, C., Gao, H. Dai, Y., Ruan, Z., Wang, J. & Sun, B. (2010). Grain refining of 409L ferritic stainless steel using Fe-Ti-N master alloy. *Metallurgical and Materials Transactions A.* 41, 1616-1620. DOI: 10.1007/s11661-010-0228-0.

[13] Park, J., Lee, C. & Park J. (2012). Effect of complex inclusion particles on the solidification structure of Fe-Ni-Mn-Mo alloy. *Metallurgical and Materials Transactions B*. 43(6), 1550-1564. DOI: 10.1007/S11663-012-9734-3.

[14] Simon, L., Jun, G., Richards, V., O'Malley, R. & Terbush, J. (2017). Optimization of melt treatment for austenitic steel grain refinement. *Metallurgical and Materials Transactions B*. 48(1), 406-419. DOI: 10.1007/S11663-016-0832-5

[15] Isobe, K. (2010). Effect of Mg addition on solidification structure of low carbon steel. *ISIJ International.* 50(12), 1972-1980. DOI: 10.2355/isijinternational.50.1972.

[16] Kivi, M. (2010). Addition of dispersoid titanium oxide inclusions in steel and their influence on grain refinement. : *Metallurgical And Materials Transactions B*. 41(6), 1194-1204. DOI: 10.1007/s11663-010-9416-y.

[17] Kivi, M. & Holappa, L. (2012). Addition of titanium oxide inclusions into liquid steel to control nonmetallic inclusions. *Metallurgical And Materials Transactions B*. 43(2), 233-240. DOI: 10.1007/S11663-011-9603-5.

[18] Bommareddy, A. & Tuttle, R.B. (2016). Study of electrolytic dissolution in steels and rare earth oxide stability. *International Journal of Metalcasting*. 10(2), 201-207. DOI: 10.1007/s40962-016-0023-9.